AIMS Mathematics, 11(3): 8655–8676.
DOI: 10.3934/math.2026356
Received: 29 January 2026
Revised: 11 March 2026
Accepted: 19 March 2026
Published: 31 March 2026

https://www.aimspress.com/journal/Math

Research article

The impact of Caputo-Fabrizio operator on the complex dynamics of a multidrug resistance model

Ahmed Ezzat Matouk[1,2,*]

[1] Department of Mathematics, College of Science Al-Zulfi, Majmaah University, Al-Majmaah, 11952, Saudi Arabia
[2] College of Engineering, Majmaah University, Al-Majmaah 11952, Saudi Arabia

* **Correspondence:** Email: ae.mohamed@mu.edu.sa.

Abstract: This work studied the impact of Caputo–Fabrizio derivatives on the chaotic dynamics in a multidrug resistance dynamical system. The local stability conditions of the drug-free, healthy, and multidrug resistance equilibrium states are proven. The numerical simulations demonstrate the presence of chaos in the considered fractional model and its integer-order counterpart, which means that the coexistence of both susceptible and infected populations is highly unpredictable because of the multidrug resistance. Furthermore, the consistency between the fractional system and its integer-order counterpart is evident for a wide time scale, despite the use of two different numerical algorithms. The new numerical algorithm for integrating the fractional model is presented, along with proofs of its conditional stability and convergence. In addition, the study used advanced software tools, such as bifurcation diagrams based on the local maxima algorithm and Lyapunov spectrum, that confirm the regions of chaos and their distribution in these systems when the growth rate of the susceptible population changes within a certain range.

Keywords: antimicrobial resistance; Caputo-Fabrizio; stability; chaos
Mathematics Subject Classification: 34H10, 34C28, 37M05

1. Introduction

Fractional calculus offers precise and effective tools for describing natural phenomena [1–3], especially those arising from economic models [4], physical models [5–7], engineering models [7–9],

epidemic models [10–12], and some interdisciplinary models that rely on the memory and the hereditary effects of fractional derivatives such as the tuberculosis disease model [13], the SEIR epidemic model [14], the COVID-19 model with vaccination efficacy [15], the Influenza model [16], the spatio-temporal SEIR epidemic model [17], the tumor model [18], and the vector-borne disease model [19]. The Caputo–Fabrizio operator (CFO) is one of the most important fractional derivatives because it contains a non-singular kernel, making it suitable for describing multiple models of interest to researchers in physics and engineering [20–22]. For example, Alqahtani et al. presented a circuit realization of a 4D dynamical system based on the CFO [23]. In addition, [24], Matouk et al. showed the existence of hidden attractors in two engineering systems using the CFO. Moreover, the CFO has appeared in several important research papers in the field of mathematical biology. For example, Khan et al. [25] investigated the dynamics of hepatitis E using the CFO. Moore et al. [26] applied the CFO to model a system for HIV with a treatment compartment. Baleanu et al. [27] examined a mathematical model for the human liver using the CFO. Peter [28] studied the transmission dynamics of the Brucellosis model using the CFO. Bonyah et al. [29] applied the CFO to model a system for coronavirus with comorbidity. In [30], the authors investigated the vector-borne disease model using the CFO. In [31], Shafqat and Alsaadi studied the bifurcation in an SIR model with normalized CFO. In [32], Shafqat et al. applied the normalized CFO to model the SVIR system.

The appearance of chaotic behaviors in an n-dimensional dynamical model is associated with high unpredictability of future behaviors of the corresponding state variables and high sensitivity to the initial conditions. To verify the existence of such interesting behaviors, the system's Lyapunov exponents (LEs or $p_m,\ m = 1,\ldots,n$) can be calculated, so that they refer to the chaotic state when their maximal (or dominant) values become positive. Hence, $p_m > 0$ indicates that the distances between the nearby trajectories are exponentially expanded over the course of time. One of the most effective algorithms that can be used to estimate the system's LEs was developed by Wolf et al. [33]. Chaos has recently emerged in many models with the CFO, such as the Newton–Leipnik model [34], financial models [35,36], the fractional-order Buck converter [37], the cancer model [38], the novel 4D system [39], and the new chaotic model given by Wang et al. [40].

Recently, global health organizations have recorded the emergence of some diseases that had previously disappeared [41]. The reasons lie in the existence of new medical factors previously unknown, such as waning vaccination, antimicrobial resistance (AMR), and multidrug resistance (MDR) [42]. One of the main explanations for these new medical factors is the excessive use of antibiotics, which over time leads to the growth of antibiotic-resistant bacteria. Therefore, many scientists and researchers have been interested in studying the AMR and MDR models; For example, Arepyeva et al. presented a model for predicting the growth of bacterial resistance [43]. Elettreby and Ahmed introduced a model of ODEs representing multi-drug AMR [44]. In [45], Ahmed et al. investigated the dynamics of a simple AMR model. In [46], Olesen studied the impact of mass drug administration of antibiotics on AMR. In [47], Durazzi et al. presented a pilot study on AMR modeling. In [48], Ahmed et al. discussed the impacts, future prospects, and challenges regarding the study of AMR. On another level, linking the memory property of fractional operators to plausible biological mechanisms in AMR has become a focal topic. It has been found that AMR modeling using fractional derivatives allows for a deeper understanding of some current observations, such as the persistence of drug resistance traits and delayed response to treatment. In [49], a simple one-drug AMR model was studied based on the Caputo fractional operator with a singular kernel. Thus, the CFO with a non-singular kernel is expected to provide better insights into the mathematics associated with AMR.

In this study, we investigate the dynamics of the two-drug AMR model using the CFO. According to the fractional Routh–Hurwitz (FRH) theory of the differential systems described by the CFO, the

stability analyses are demonstrated for the system's equilibrium solutions. For this reason, four proven lemmas are presented to analyze the local stability of the drug-free, healthy, and multidrug resistance equilibrium points. Some numerical results are obtained via the fourth-order Runge–Kutta (fourth-order RK) scheme that integrates the integer-order system, and a novel method that integrates the fractional-order models in the CFO sense. The conditional stability and convergence of the proposed numerical scheme are proved. The consistency of these numerical results is evident because the chaotic attractors are similar and almost coincide over a large time, in both the fractional system and its integer-order counterpart, despite the use of two different numerical algorithms. In addition, the study used the bifurcation diagrams and Lyapunov spectrum to examine the regions of chaos and their distribution in these systems when the growth rate of the susceptible population changes within a certain range. Therefore, this study provides useful tools to model, predict, estimate, and control the complex dynamics of some viral diseases, especially when their recurrences are associated with MDR.

2. Fractional calculus

The CFO is defined as

$$ {}^{Cf}_{t}D^{q}_{a}u(t)=\begin{cases}\dfrac{\mathrm{M}(q)}{1-q}\displaystyle\int_{a}^{t}\frac{du(\tau)}{d\tau}\exp[-\frac{q}{1-q}(t-\tau)]d\tau, & 0<q<1,\\ \dfrac{du(t)}{dt}, & q=1,\end{cases} \tag{1}$$

where q and $\mathrm{M}(q)$ represent the fractional-order and the normalization function, respectively. The normalization function must equal one when the fractional-order is vanished or equals one. The corresponding fractional integral is given by

$$ {}^{Cf}\mathrm{I}^{q}_{a}u(t)=(1-q)u(t)+q\int_{a}^{t}u(\tau)d\tau. \tag{2}$$

The CFO is also subject to the following characteristics [50,51]:

1) If $u\in C^{k}([\alpha,\beta]),k=1,2,3,...,$ then

$$\frac{d^{k}}{dt^{k}}{}^{Cf}_{0}D^{q}_{t}u(t)=\sum_{l=1}^{k}(-1)^{k-l}\frac{q^{k-l}}{(1-q)^{k-l+1}}u^{(l)}(t)+(-1)^{k}(\frac{q}{1-q})^{k}{}^{Cf}_{0}D^{q}_{t}u(t).$$

2) If $u\in C^{1}([\alpha,\beta]),$ then ${}^{Cf}_{0}D^{q}_{t}u(t)\in C^{1}([\alpha,\beta]).$

3) The CFO ${}^{Cf}_{0}D^{q}_{t}:C^{1}([\alpha,\beta])\to C^{1}([\alpha,\beta])$ is a bounded operator, which satisfies

$$\left\|{}^{Cf}_{0}D^{q}_{t}u\right\|_{C^{1}([\alpha,\beta])}\le\frac{1}{q}\left(1-e^{\frac{q(\beta-\alpha)}{q-1}}\right)\|u\|_{C^{1}([\alpha,\beta])}.$$

4) If $u(t)\in H^{1}(\alpha,\beta),$ then ${}^{Cf}_{0}D^{q}_{t}u(t)\in L^{2}(\alpha,\beta).$

Consider the general system

$$\begin{aligned}&{}^{Cf}_{t}D^{q}_{0}\mathrm{X}(t)=J\mathrm{X}(t)+f(t,\mathrm{X}),\ q\in(0,1),\\&\mathrm{X}(0)=\mathrm{X}_{0},\end{aligned} \tag{3}$$

where $0 < q < 1$, $\mathrm{X}(t) \in R^4$, $f : [0,\infty) \times R^4 \to R^4$, and J is a 4×4 scalar matrix. Then, the matrix $J(\overline{\mathrm{X}})$ can be defined as the Jacobian of the linearized form of Eq (3), where $\overline{\mathrm{X}}$ represents the related equilibrium solution. So, the following results hold:

Lemma 1. [52] Assume that the matrix $\mathrm{M} = \left(I_4 + (q-1)J\right)$ is a non-singular, μ_i, $i = 1,2,3,4$ represents an arbitrary eigenvalue of J, and $\mu(q\mathrm{M}J)$ represents an eigenvalue of the matrix $q\mathrm{M}J$. The equilibrium solution $\overline{\mathrm{X}}$ is locally asymptotically stable (LAS) if and only if

$$\mu_i(q\mathrm{M}J) = \frac{q}{1-q}\left(\frac{1}{1+\mu_i(q-1)} - 1\right) \text{ for all } i = 1,2,3,4.$$

Lemma 2. [52] Assume that the eigenvalues of $J(\overline{\mathrm{X}})$ have the form $\mu_{1,2} = \alpha \pm j\beta$, $j = \sqrt{-1}$, $\mu_3 < 0$ and $\mu_4 < 0$. If M is non-singular, then $\overline{\mathrm{X}}$ is LAS if and only if $\mu_i \notin C(q) \forall i = 1,2,$ where

$$C(q) = \left\{(\alpha,\beta) \in R^2 \middle| (\alpha - \frac{1}{2(1-q)})^2 + \beta^2 = \frac{1}{4(1-q)^2}\right\}. \tag{4}$$

Lemma 3. [53] Assume that M is non-singular and $a_{im} \in J(\overline{\mathrm{X}})$ such that $a_{ii} = \frac{1}{2-2q} \forall i = 1,2,3,4$. If

$$\sum_{m=1, m\neq i}^{4} |a_{im}| > \frac{1}{1-q},$$

then $\overline{\mathrm{X}}$ is LAS. Otherwise, if

$$\sum_{m=1, m\neq i}^{4} |a_{im}| < \frac{1}{1-q},$$

then $\overline{\mathrm{X}}$ is unstable.

Theorem 1. Suppose that $\mu_i \in R$ for all $i = 1,2,3,4$. The equilibrium state $\overline{\mathrm{X}}$ of system (3) is LAS if and only if $\mu_i > \frac{1}{1-q}$ or $\mu_i < 0$.

Proof. According to Lemma 1, the general system (3) has the following eigenvalue:

$$\mu(q\mathrm{M}J) = \frac{q}{1-q}\left(\frac{1}{1+\mu(q-1)} - 1\right).$$

Obviously, the quantity $\frac{1}{1+\mu(q-1)} - 1$ is negative if and only if ($\mu < 0$) or ($\mu > 0, 1+\mu(q-1) < 0$). Then, we have two cases; the first case, $\mu < 0$, provides a sufficient condition for $\overline{\mathrm{X}}$ to be LAS according to Lemma 1. The second case, $\mu > 0, 1+\mu(q-1) < 0$, is equivalent to $\mu > \frac{1}{1-q}$, which provides a sufficient condition for $\overline{\mathrm{X}}$ to be LAS according to Lemma 1.

Remark 1. If all the coefficients of the characteristic equation of system (3) satisfy the classic Routh–Hurwitz criterion, then $\overline{\mathrm{X}}$ is LAS.

3. Describing the two-drug AMR systems

The dynamics of four types of susceptible and infected populations that resist two kinds of antimicrobial drugs A and B can be investigated via the following two-drug AMR model [44]:

$$\begin{aligned}
\frac{dx}{dt} &= (r(1-x) - \gamma_1 y - \gamma_2 z - \gamma_3 w)x, \\
\frac{dy}{dt} &= (-\sigma_1 + \gamma_1 x - \gamma_4 w)y, \\
\frac{dz}{dt} &= (-\sigma_2 + \gamma_2 x - \gamma_5 w)z, \\
\frac{dw}{dt} &= (-\sigma_3 + \gamma_3 x + \gamma_4 y + \gamma_5 z)w,
\end{aligned} \tag{5}$$

where the susceptible population is represented by x and the infected population that only responds to drug A is represented by y. The infected population that only responds to drug B is represented by z. Finally, we use the variable w to represent the infected population that resists both of these vaccines. The parameter $r > 0$ indicates the rate of growth of x. The positive parameters $\sigma_1, \sigma_2, \sigma_3$ represent the natural death rate of y, z, and w, respectively. The positive parameters $\gamma_1, \gamma_2, \gamma_3$ represent the encounter rate of x with y, x with z, and x with w for each unit time, respectively. The encounter rate of y with w per unit time is denoted by γ_4, and the encounter rate of z with w per unit time is denoted by γ_5. Throughout this work, all parameters of the system are arranged in the set $\Omega = \{r, \gamma_1, \gamma_2, \gamma_3, \gamma_4, \gamma_5, \sigma_1, \sigma_2, \sigma_3\}$.

The corresponding model governed by the CFO can be suggested as

$$\begin{aligned}
{}^{Cf}D_0^q x(t) &= (r'^q(1-x) - \gamma_1'^q y - \gamma_2'^q z - \gamma_3'^q w)x, \\
{}^{Cf}D_0^q y(t) &= (-\sigma_1'^q + \gamma_1'^q x - \gamma_4'^q w)y, \\
{}^{Cf}D_0^q z(t) &= (-\sigma_2'^q + \gamma_2'^q x - \gamma_5'^q w)z, \\
{}^{Cf}D_0^q w(t) &= (-\sigma_3'^q + \gamma_3'^q x + \gamma_3'^q y + \gamma_5'^q z)w,
\end{aligned}$$

where $0 < q < 1$. The operator ${}^{Cf}D_0^q$ has the dimension of $1/t^q$, where t refers to the time. Therefore, all the parameters in this fractional-order model have exponents of q. Essentially, all the parameters of this fractional model have dimensions of $1/t^q$ and can be rewritten as

$$r = r'^q, \gamma_i = \gamma_i'^q, (i = 1,2,3,4,5), \sigma_k = \sigma_k'^q, (k = 1,2,3).$$

So, the fractional-order two-drug AMR system governed by the CFO becomes

$$\begin{aligned}
{}^{Cf}D_0^q x(t) &= (r(1-x) - \gamma_1 y - \gamma_2 z - \gamma_3 w)x, \\
{}^{Cf}D_0^q y(t) &= (-\sigma_1 + \gamma_1 x - \gamma_4 w)y, \\
{}^{Cf}D_0^q z(t) &= (-\sigma_2 + \gamma_2 x - \gamma_5 w)z, \\
{}^{Cf}D_0^q w(t) &= (-\sigma_3 + \gamma_3 x + \gamma_4 y + \gamma_5 z)w.
\end{aligned} \tag{6}$$

Here, the fractional parameter q is said to be the memory parameter because it illustrates the impact

of prior experiences on the current populations' behaviors, which makes the fractional system have better accuracy to the actual data than the integer-order counterpart.

The system (6) has the equilibrium states:

$$\begin{aligned}&\overline{\mathrm{X}}_0=(0,0,0,0),\ \overline{\mathrm{X}}_1=(1,0,0,0),\ \overline{\mathrm{X}}_2=(\eta_1,\theta_1,0,0),\ \overline{\mathrm{X}}_3=(\eta_2,0,\theta_2,0),\\&\overline{\mathrm{X}}_4=(\eta_3,0,0,\theta_3),\ \overline{\mathrm{X}}_5=(\nu_1,\nu_2,0,\nu_3),\ \overline{\mathrm{X}}_6=(\tilde{\nu}_1,0,\tilde{\nu}_2,\tilde{\nu}_3),\ \overline{\mathrm{X}}_7=(\lambda_1,\lambda_2,\lambda_3,\lambda_4),\end{aligned}\tag{7}$$

where

$$\begin{aligned}&\eta_1=\frac{\sigma_1}{\gamma_1},\ \eta_2=\frac{\sigma_2}{\gamma_2},\ \eta_3=\frac{\sigma_3}{\gamma_3},\ \theta_1=\frac{r}{\gamma_1}(1-\frac{\sigma_1}{\gamma_1}),\ \theta_2=\frac{r}{\gamma_2}(1-\frac{\sigma_2}{\gamma_2}),\ \theta_3=\frac{r}{\gamma_3}(1-\frac{\sigma_3}{\gamma_3}),\\&\nu_1=1-\frac{\gamma_1\sigma_3-\gamma_3\sigma_1}{r\gamma_4},\ \tilde{\nu}_1=1-\frac{\gamma_2\sigma_3-\gamma_3\sigma_2}{r\gamma_5},\ \nu_2=\frac{\sigma_3-\gamma_3\nu_1}{\gamma_4},\ \tilde{\nu}_2=\frac{\sigma_3-\gamma_3\tilde{\nu}_1}{\gamma_5},\\&\nu_3=\frac{\gamma_1\nu_1-\sigma_1}{\gamma_4},\ \tilde{\nu}_3=\frac{\gamma_2\tilde{\nu}_1-\sigma_2}{\gamma_5},\ \lambda_1=\frac{\gamma_5\sigma_1-\gamma_4\sigma_2}{\gamma_1\gamma_5-\gamma_2\gamma_4},\ \lambda_2=\frac{\gamma_2(\gamma_3\lambda_1-\sigma_3)+\gamma_5(r(1-\lambda_1)-\gamma_3\lambda_4)}{\gamma_1\gamma_5-\gamma_2\gamma_4},\\&\lambda_3=-\frac{\gamma_1(\gamma_3\lambda_1-\sigma_3)+\gamma_4(r(1-\lambda_1)-\gamma_3\lambda_4)}{\gamma_1\gamma_5-\gamma_2\gamma_4},\ \lambda_4=\frac{\gamma_2\sigma_1-\gamma_1\sigma_2}{\gamma_1\gamma_5-\gamma_2\gamma_4},\end{aligned}$$

where $\eta_i,\theta_i,\nu_i,\tilde{\nu}_i>0,\ i=1,2,3$ and $\lambda_k>0,k=1,2,3,4.$

4. Stability conditions

In the following, the stability of the equilibrium states (7) will be examined. Throughout this section, we assume that $Det(\mathrm{M})\neq 0,$ where $\mathrm{M}=\left(I_4+(q-1)J(\overline{\mathrm{X}})\right)$ for any arbitrary equilibrium point $\overline{\mathrm{X}}$, which implies that the matrix M is non-singular. First, we examine the stability of the trivial (drug-free) equilibrium state $\overline{\mathrm{X}}_0$, which has the eigenvalues $\mu_1=r,\mu_2=-\sigma_1,\mu_3=-\sigma_2$ and $\mu_4=-\sigma_3.$ According to Theorem 1, $\overline{\mathrm{X}}_0$ is LAS when $q<1-\frac{1}{r}.$ In addition, the healthy (axial) state $\overline{\mathrm{X}}_1$ has the eigenvalues $\mu_1=-r,\mu_2=\gamma_1-\sigma_1,\mu_3=\gamma_2-\sigma_2$ and $\mu_4=\gamma_3-\sigma_3.$ So, according to Theorem 1, the healthy state $\overline{\mathrm{X}}_1$ is LAS if and only if $(\sigma_i>\gamma_i,i=1,2,3)$ or $(\gamma_i>\frac{1+\sigma_i(1-q)}{1-q},\ i=1,2,3).$

Second, to maintain the physical meaning of the model, we will focus on studying the stability of equilibrium states in which the fourth component does not vanish, so that the effect of MDR remains present.

The stability conditions of $\overline{\mathrm{X}}_4$ are presented below.

Lemma 4. Assume that $Det(\mathrm{M})\neq 0,$ the equilibrium solution $\overline{\mathrm{X}}_4=(\eta_3,0,0,\theta_3)$ is LAS if and only if at least one of the following statements is true:

(i) $\theta_3>\max(\frac{\gamma_1\eta_3-\sigma_1}{\gamma_4},\frac{\gamma_2\eta_3-\sigma_2}{\gamma_5})$ when $\theta_3\leq\frac{\eta_3^2r^2}{4\gamma_3\sigma_3}.$

(ii) $\theta_3<(1-q)\min(\frac{\gamma_1\eta_3-\sigma_1}{\gamma_4},\frac{\gamma_2\eta_3-\sigma_2}{\gamma_5})$ when $\theta_3\leq\frac{\eta_3^2r^2}{4\gamma_3\sigma_3}.$

(iii) $\theta_3 > \max(\frac{\gamma_1\eta_3 - \sigma_1}{\gamma_4}, \frac{\gamma_2\eta_3 - \sigma_2}{\gamma_5})$ when $\theta_3 > \frac{\eta_3^2 r^2}{4\gamma_3\sigma_3}$.

Proof. The eigenvalues of $\overline{\mathrm{X}}_4 = (\eta_3, 0, 0, \theta_3)$ that correspond to the matrix J satisfy the equation

$$\begin{aligned} &P(\mu) = (\mu - \gamma_1\eta_3 + \sigma_1 + \gamma_4\theta_3)(\mu^3 + s_1\mu^2 + s_2\mu + s_3) = 0, \\ &s_1 = \gamma_5\theta_3 + \sigma_2 + \eta_3(r - \gamma_2), \\ &s_2 = \eta_3(r\gamma_5\theta_3 - r\gamma_2\eta_3 + r\sigma_2 + \gamma_3^2\theta_3), \\ &s_3 = \gamma_3^2\theta_3\eta_3(\sigma_2 - \gamma_2\eta_3 + \gamma_5\theta_3). \end{aligned} \tag{8}$$

Equation (8) has the following roots:

$$\mu_1 = \gamma_1\eta_3 - \sigma_1 - \gamma_4\theta_3, \mu_2 = \gamma_2\eta_3 - \sigma_2 - \gamma_5\theta_3 \text{ and } \mu_{3,4} = \frac{-\eta_3 r \pm \sqrt{\eta_3^2 r^2 - 4\gamma_3\sigma_3\theta_3}}{2}. \tag{9}$$

The condition $\theta_3 \le \frac{\eta_3^2 r^2}{4\gamma_3\sigma_3}$ implies that $\mu_{3,4} < 0$. Then, according to Theorem 1, $\overline{\mathrm{X}}_4$ is LAS iff

$$\theta_3 > \max(\frac{\gamma_1\eta_3 - \sigma_1}{\gamma_4}, \frac{\gamma_2\eta_3 - \sigma_2}{\gamma_5}) \text{ or } \theta_3 < (1-q)\min(\frac{\gamma_1\eta_3 - \sigma_1}{\gamma_4}, \frac{\gamma_2\eta_3 - \sigma_2}{\gamma_5}).$$

However, the condition $\theta_3 > \frac{\eta_3^2 r^2}{4\gamma_3\sigma_3}$ implies that the eigenvalues $\mu_{3,4}$ are two complex conjugates. Then, according to Lemma 2, $\overline{\mathrm{X}}_4$ is LAS iff

$$\theta_3 > \max(\frac{\gamma_1\eta_3 - \sigma_1}{\gamma_4}, \frac{\gamma_2\eta_3 - \sigma_2}{\gamma_5}).$$

Lemma 5. Assume that $Det(\mathrm{M}) \neq 0$, the equilibrium solution $\overline{\mathrm{X}}_5 = (\nu_1, \nu_2, 0, \nu_3)$ exists when

$$r(1-\eta_3) < \frac{\gamma_1\sigma_3 - \gamma_3\sigma_1}{\gamma_4} < r(1 - \frac{\sigma_1}{\gamma_1}). \tag{10}$$

It is LAS if $\gamma_2\nu_1 - \gamma_5\nu_3 - \sigma_2 < 0$ or $\gamma_2\nu_1 - \gamma_5\nu_3 - \sigma_2 > \frac{1}{1-q}$.

Proof. When the inequality (10) holds, the eigenvalues of $\overline{\mathrm{X}}_5$ that correspond to the matrix J satisfy the equation

$$P_1(\mu)(\mu + \gamma_5\nu_3 + \sigma_2 - \gamma_2\nu_1) = 0, \tag{11}$$

where

$$P_1(\mu) = \mu^3 + s_1'\mu^2 + s_2'\mu + s_3', \quad s_1' = \nu_1 r, \; s_2' = \nu_1\nu_3\gamma_3^2 + \nu_1\nu_2\gamma_1^2 + \nu_2\nu_3\gamma_4^2, \; s_3' = r\nu_1\nu_2\nu_3\gamma_4^2.$$

It is clear that $s_i' > 0 \forall i = 1,2,3$ and fulfills the classic Routh–Hurwitz criterion,

$$s_1' > 0, \; s_3' > 0, \; s_1's_2' - s_3' > 0,$$

which implies that all the roots of $P_1(\mu)$ have negative real parts. According to Theorem 1 and Remark 1, $\overline{\mathrm{X}}_5$ is LAS if the fourth eigenvalue of $\overline{\mathrm{X}}_5$, $\mu_4 = \gamma_2\nu_1 - \gamma_5\nu_3 - \sigma_2$ is negative or satisfies the inequality $\gamma_2\nu_1 - \gamma_5\nu_3 - \sigma_2 > \frac{1}{1-q}$.

Lemma 6. Assume that $Det(\mathrm{M}) \neq 0$, the multidrug resistance solution $\overline{\mathrm{X}}_6 = (\tilde{\nu}_1, 0, \tilde{\nu}_2, \tilde{\nu}_3)$ exists when

$$r(1-\eta_3) < \frac{\gamma_2\sigma_3 - \gamma_3\sigma_2}{\gamma_5} < r(1-\frac{\sigma_2}{\gamma_2}). \tag{12}$$

The following statements are obtained:

(i) When $D(P_2(\mu)) > 0$, and one of the conditions $\gamma_1\tilde{\nu}_1 - \sigma_1 - \gamma_4\tilde{\nu}_3 < 0$ or $\gamma_1\tilde{\nu}_1 - \sigma_1 - \gamma_4\tilde{\nu}_3 > \frac{1}{1-q}$ holds, then $\overline{\mathrm{X}}_6$ is LAS if either the conditions ($c_1 > 0$, $c_2 > 0$, $\gamma_3 > 0$) or ($c_1 > 0$, $c_3 > 0$, $c_1c_2 - c_3 > 0$) hold true;

(ii) When $D(P_2(\mu)) < 0$, and one of the conditions $\gamma_1\tilde{\nu}_1 - \sigma_1 - \gamma_4\tilde{\nu}_3 < 0$ or $\gamma_1\tilde{\nu}_1 - \sigma_1 - \gamma_4\tilde{\nu}_3 > \frac{1}{1-q}$ holds, then $\overline{\mathrm{X}}_6$ is LAS if either the conditions ($c_1 > 0$, $c_2 > 0$, $\gamma_3 > 0$, $c_1c_2 = c_3$) or ($\rho > \frac{1}{1-q}$, $P_2(\mu)P_2(\frac{1}{1-q}) < 0$, $c_3 < -\frac{\rho}{(1-q)^2}$, $c_1 < 0$, $c_2 > 0$, $c_3 < 0$) hold true;

(iii) When $D(P_2(\mu)) < 0$, then $\overline{\mathrm{X}}_6$ is unstable if either the conditions ($c_1 < 0$, $c_2 > 0$, $c_3 < 0$, $\rho < \frac{1}{1-q}$) or ($c_1 > 0$, $c_2 > 0$, $c_1c_2 < c_3 < \frac{c_1}{(1-q)^2}$) hold true;

(iv) When $D(P_2(\mu)) > 0$, $c_1 < 0$, $c_2 > 0$, $c_3 < 0$, and $|c_3| < 1$, then $\overline{\mathrm{X}}_6$ is unstable,

where $D(P_2(\mu))$ represents the discriminant of the polynomial

$$P_2(\mu) = \mu^3 + c_1\mu^2 + c_2\mu + c_3, \tag{13}$$

$$c_1 = r - \frac{\gamma_2\sigma_3 - \gamma_3\sigma_2}{\gamma_5},$$

$$\begin{aligned} c_2 = &-\frac{r^2}{\gamma_5}[(\sigma_2-\gamma_2)(\gamma_3^2+\sigma_3\gamma_5-\gamma_5\gamma_3)+\gamma_2^2(\gamma_3-\sigma_3)] - \frac{r}{\gamma_5^3}[-2\gamma_2\gamma_5\gamma_3(\gamma_2^2\sigma_3+\gamma_3^2\sigma_2) \\ &+(\gamma_2+\gamma_5)(\gamma_2^2\sigma_3^2\gamma_5+2\gamma_2\gamma_5\gamma_3^2\sigma_2)+(\gamma_3-\gamma_5)(\sigma_2^2\gamma_5\gamma_3^2+2\gamma_2^2\gamma_3\gamma_5\sigma_3)-\sigma_2\sigma_3\gamma_2\gamma_5\gamma_3(\gamma_2+\gamma_3)] \\ &-\frac{1}{\gamma_5^3}[(\gamma_2-\gamma_3)(\gamma_3\gamma_2^3\sigma_3^2-2\gamma_2^2\sigma_3\gamma_3^2\sigma_2)+\gamma_3^3\gamma_2\sigma_2^2(\gamma_2+\gamma_5-\gamma_3)+\gamma_5\sigma_3\gamma_2^2\gamma_3(\gamma_2\sigma_3-2\gamma_3\sigma_2)], \end{aligned}$$

$$c_3 = r^3(\sigma_2-\gamma_2)(\gamma_3-\sigma_3)+\frac{r^2}{\gamma_5}(\sigma_3\gamma_2-\sigma_2\gamma_3)[\sigma_3\sigma_2+3\gamma_2\gamma_3-2(\sigma_3\gamma_2+\sigma_2\gamma_3)]$$
$$\frac{-3\gamma_2\gamma_3 r(\gamma_3^2\sigma_2^2+\gamma_2^2\sigma_3^2)-\gamma_2\gamma_3\sigma_2\sigma_3 r(\sigma_3\gamma_2+\sigma_2\gamma_3)+6\gamma_2^2\gamma_3^2\sigma_3\sigma_2 r+\gamma_3^3\sigma_2^3 r+\gamma_2^3\sigma_3^3 r}{b_5^2}$$
$$+\frac{3\gamma_2^2\gamma_3^2\sigma_2\sigma_3(\sigma_2\gamma_3-\sigma_3\gamma_2)+\gamma_2\gamma_3(\gamma_2^3\sigma_3^3-\gamma_3^3\sigma_2^3)}{\gamma_5^3},$$

and $\rho = \max(-c_3,-c_2,-c_1)+1.$

Proof. When the inequality (12) holds, the eigenvalues of $\overline{\mathrm{X}}_6$ that correspond to the matrix J satisfy the equation

$$\mu_4 P_2(\mu) = 0, \tag{14}$$

where $\mu_4 = \gamma_1\tilde{\nu}_1 - \sigma_1 - \gamma_4\tilde{\nu}_3 - \mu$. According to Theorem 1, the conditions $\mu_4 < 0$ or $\mu_4 > \frac{1}{1-q}$ imply that the eigenvalue μ_4 lies in the stable region.

Assuming that μ_4 satisfies the previous stability inequalities, and recalling the local stability statement in condition (I) of Theorem 1 [53], when $D(P_2(\mu)) > 0,$ the equilibrium point is LAS if ($c_i > 0,\ i = 1,2,3$) or if the classic Routh–Hurwitz conditions hold. So, part (i) is proved.

Assume that μ_4 satisfies the previous stability inequalities. Recalling condition (II) of Theorem 1 [53], when $D(P_2(\mu)) < 0,$ the equilibrium point is LAS if $c_i > 0,\ i = 1,2,3$ and $c_1c_2 = c_3$. In addition, recalling the local stability statement in condition (III) of Theorem 1 [53], when $D(P_2(\mu)) < 0,$ the equilibrium point is LAS if $c_1 < 0$, $c_2 > 0$, $c_3 < 0$, $\rho > \frac{1}{1-q}$, $P_2(\mu)P_2(\frac{1}{1-q}) < 0$, and $c_3 < -\frac{\rho}{(1-q)^2}$. This completes the proof of part (ii).

Recalling the unstability statement in condition (III) of Theorem 1 [53], when $D(P_2(\mu)) < 0,$ the equilibrium point is unstable if $c_1 < 0$, $c_2 > 0$, $c_3 < 0$, and $\rho < \frac{1}{1-q}$. Recalling the condition (IV) of Theorem 1 [53], when $D(P_2(\mu)) > 0,$ the equilibrium point is unstable if $c_1 > 0$, $c_2 > 0$, and $c_1c_2 < c_3 < \frac{c_1}{(1-q)^2}$. Part (iii) is now proved.

Recalling the unstability statement in condition (I) of Theorem 1 [53], when $D(P_2(\mu)) > 0,$ the equilibrium point is unstable if $c_1 < 0$, $c_2 > 0$, $c_3 < 0$, and $|c_3| < 1$. This completes the proof of part (iv).

Lemma 7. Assume that $Det(\mathrm{M}) \neq 0$ and $\gamma_1\gamma_5 > \gamma_2\gamma_4$; the multidrug resistance solution $\overline{\mathrm{X}}_7 = (\lambda_1,\lambda_2,\lambda_3,\lambda_4)$ satisfies the following statements:

(i) If $D(P_3(\mu)) < 0$ and $\frac{c_3'}{c_1'c_2'} = 1 - \frac{c_1'c_4'}{c_2'c_3'}$, then $\overline{\mathrm{X}}_7$ is LAS;

(ii) If $D(P_3(\mu)) > 0$, $P_3(l_1)P_3(0) < 0$, and $l_2 < 0$, then $\overline{\mathrm{X}}_7$ is LAS;

(iii) If $D(P_3(\mu)) > 0$, $P_3(l_2)P_3(\frac{1}{1-q}) < 0$, and $l_1 > \frac{1}{1-q}$, then $\overline{\mathrm{X}}_7$ is LAS;

(iv) If $c_1'c_2' > c_3'$ and $c_1'c_2'c_3' = c_4'c_1'^2 + c_3'^2$, then $\overline{\mathrm{X}}_7$ is LAS,

where $D(P_3(\mu))$ represents the discriminant of

$$D(P_3(\mu)) = \mu^4 + c_1'\mu^3 + c_2'\mu^2 + c_3'\mu + c_4' = 0, \tag{15}$$

$$\begin{aligned} c_1' &= r\lambda_1 > 0, \\ c_2' &= \lambda_2\gamma_4^2 + \lambda_3\gamma_5^2 + \lambda_1(\lambda_2\gamma_1^2 + \lambda_3\gamma_2^2 + \lambda_4\gamma_3^2) > 0, \\ c_3' &= r\lambda_1\lambda_4(\lambda_2\gamma_4^2 + \lambda_3\gamma_5^2) > 0, \\ c_4' &= \lambda_1\lambda_2\lambda_3\lambda_4(\gamma_2^2\gamma_4^2 + \gamma_1^2\gamma_5^2 - \gamma_1\gamma_2\gamma_4\gamma_5) > 0, \end{aligned}$$

$$l_1 = -\frac{c_1'}{4} - \frac{3}{4}\sqrt{(c_1')^2 - \frac{8c_2'}{3}} \quad \textit{and} \quad l_2 = -\frac{c_1'}{4} + \frac{3}{4}\sqrt{(c_1')^2 - \frac{8c_2'}{3}}.$$

Proof. Recalling the condition (III) of Theorem 2 [53], when $D(P_3(\mu)) < 0,$ the equilibrium point is LAS if $\frac{c_3'}{c_1'c_2'} = 1 - \frac{c_1'c_4'}{c_2'c_3'}$ and $c_i', i = 1,2,3,4$. Part (i) is now proved.

Recalling the first statement in condition (VI) of Theorem 2 [53], when $D(P_3(\mu)) > 0,$ the equilibrium point is LAS if $P_3(l_1)P_3(0) < 0$ and $l_2 < 0$. This proves part (ii).

Recalling the second statement in condition (VI) of Theorem 2 [53], when $D(P_3(\mu)) > 0,$ the equilibrium point is LAS if $P_3(l_2)P_3(\frac{1}{1-q}) < 0$ and $l_1 > \frac{1}{1-q}$. This completes the proof of part (iii).

Recalling the condition (VII) of Theorem 2 [53], if $c_1' > 0, c_2' > 0,$ $c_1'c_2' > c_3'$, and $c_1'c_2'c_3' = c_4'c_1'^2 + c_3'^2$, then the equilibrium point is LAS. The proof of part (iv) is now completed.

5. Numerical simulations

5.1. The integer-order system (5)

Based on the fourth-order RK scheme, system (5) possesses a chaotic attractor when $x(0) = 0.15, y(0) = 0.15, z(0) = 0.4, w(0) = 10^{-15}$ and using $\Omega^{(1)} = \{3,17.5,2,75,1,10.3,1,0.1,11.5\}$ as illustrated in Figure 1. In addition, we use the parameter set $\Omega_r^{(1)} = \{r,17.5,2,75,1,10.3,1,0.1,11.5\}, r > 0$ and the above-mentioned initial conditions to obtain a bifurcation diagram for system (5). In Figure 2, the bifurcation diagram, based on the local maxima (LM) algorithm, shows wide regions of chaotic behaviors. This highlights the importance of exploring these chaotic regions because they mean that the coexistence of both susceptible and infected populations is highly unpredictable because of the multidrug resistance.

The system's LEs (p_m, $m = 1,2,3,4$) are calculated according to [33], and their spectrum is drawn in Figure 3 as the susceptible population's growth rate varies between 2 and 3. The calculations show

that the coexistence of both susceptible and infected populations is highly unpredictable when the susceptible population's growth rate is greater than 2.2. When r drops further to 2.2, the coexistence of both susceptible and infected populations gradually becomes predictable (chaos is suppressed).

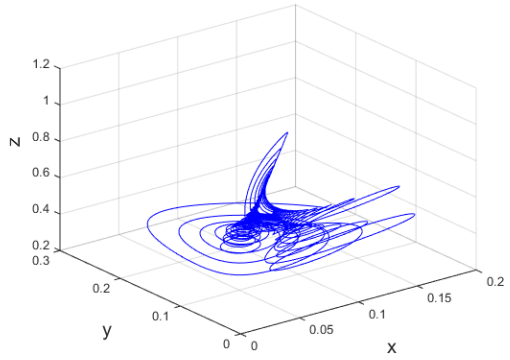

Figure 1. Chaotic attractor of the two-drug AMR system (5).

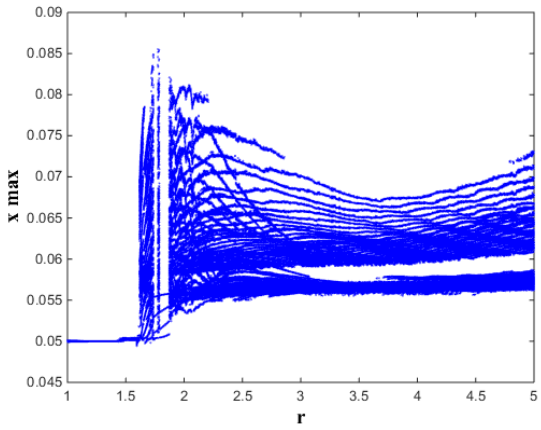

Figure 2. LM bifurcation diagram of the two-drug AMR model (5) shown using $\Omega_r^{(1)}$.

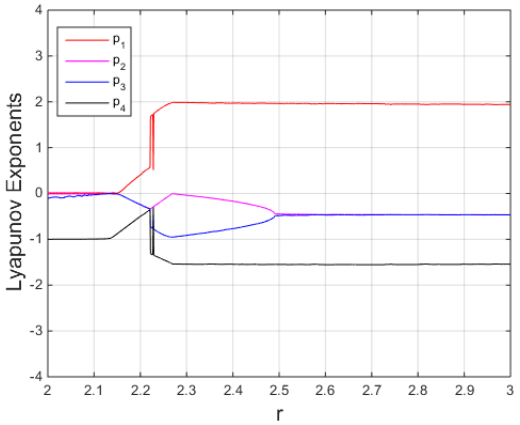

Figure 3. Lyapunov spectrum of the two-drug AMR system (5) shown using $\Omega_r^{(1)}$.

5.2. The fractional-order system (6)

The system (6) is numerically integrated using a new numerical algorithm that reformulates the system to the following form:

$$ {}^{Cf}_{t}D^{q}_{0}\mathrm{X}(t) = f(t,\mathrm{X}(t)),\ \ \mathrm{X}(0) = \mathrm{X}_0. \tag{16} $$

In the following, we consider that $\forall \mathrm{X} \in R^4$, the norm

$$ \|\xi\| = \max_{0\le t\le T}\left|\sum_{l=1}^{4}\mathrm{X}_l(t)\right| $$

is defined in the Banach space $\mathrm{B} = \Phi\times\Phi\times\Phi\times\Phi$, such that $\Phi = C[0,T]$. In addition, we will use the following Lipschitz hypotheses:

H1: $\forall \mathrm{X}\in \mathrm{B}$, there exists $L>0$ and a constant κ such that $\left|f(t,\mathrm{X}(t)\right| \le L\left|\mathrm{X}(t)\right| + \kappa$, where L represents the Lipschitz constant.

H2: $\forall \mathrm{X}, \mathrm{X}' \in \mathrm{B}$, there exists a constant $L>0$ such that $\left|f(t,\mathrm{X}(t) - f(t,\mathrm{X}'(t)\right| \le L\left|\mathrm{X}(t) - \mathrm{X}'(t)\right|$.

According to Proposition 3 in [54], the solution of system (16) is rewritten as

$$ \mathrm{X}(t) = \mathrm{X}_0 + {}^{Cf}\mathrm{I}^{q}_{a} f(\mathrm{X}(t)),\ a<t<b<\infty, $$

where the operator ${}^{Cf}\mathrm{I}^{q}_{a} : \mathrm{B}\to\mathrm{B}$ is defined in Eq (2). So, we get

$$ \mathrm{X}(t) = \mathrm{X}_0 + f(t,\mathrm{X}(t))(1-q) + q\int_{a}^{t} f(\tau,\mathrm{X}(\tau))d\tau. \tag{17} $$

Then, a discrete form of Eq (17) is presented as

$$ \mathrm{X}(t_{s+1}) = \mathrm{X}_0 + (1-q)f(t_s,\mathrm{X}(t_s)) + q\int_{a}^{t_{s+1}} f(t,\mathrm{X}(t))dt, \tag{18} $$

where $s\in\{0\}\cup Z^{+}$. The previous equation is represented as

$$ \mathrm{X}(t_s) = \mathrm{X}_0 + (1-q)f(t_{s-1},\mathrm{X}(t_{s-1})) + q\int_{a}^{t_s} f(t,\mathrm{X}(t))dt. \tag{19} $$

Utilizing Eqs (18) and (19), we get

$$ \mathrm{X}(t_{s+1}) = \mathrm{X}(t_s) + (1-q)\left[f(t_s,\mathrm{X}(t_s)) - f(t_{s-1},\mathrm{X}(t_{s-1}))\right] + q\int_{t_s}^{t_{s+1}} f(t,\mathrm{X}(t))dt, \tag{20} $$

and

$$ \int_{t_s}^{t_{s+1}} f(t,\mathrm{X}(t))dt = \left(1.5f(t_s,\mathrm{X}_s) - 0.5f(t_{s-1},t_{s-1})\right)h, \tag{21} $$

where h refers to the step size of this algorithm. Finally, we get

$$\mathrm{X}(t_{s+1}) = \mathrm{X}(t_s) + \left[1.5qh + (1-q)\right] f(t_s, \mathrm{X}_s) - \left[0.5qh + (1-q)\right] f(t_{s-1}, \mathrm{X}_{s-1}). \tag{22}$$

Equation (22) is rewritten as

$$\mathrm{X}(t_{s+1}) = \mathrm{X}_0 + \left[0.5qh + (1-q)\right] f(t_s, \mathrm{X}_s) + qh \sum_{l=0}^{s} f(t_l, \mathrm{X}_l). \tag{23}$$

Comparing Eqs (18) and (23), the error E of this algorithm can be obtained from

$$E = q\left| \int_a^b f(t, \mathrm{X}(t))dt - (0.5hf(t_s, \mathrm{X}_s) + h\sum_{l=0}^{s} f(t_l, \mathrm{X}_l)) \right|, \tag{24}$$

where $h = \dfrac{b-a}{N}$ and $t_l = a + hl,\ l = 0,1,...,s$ on $[a,b]$. Then, in light of Eq (21) and the Taylor series, the integrand function is expanded about t_0 as follows:

$$\int_{t_0}^{t_0+h} f(t, \mathrm{X}(t))dt = \int_{t_0}^{t_0+h} \left(f(t_0, \mathrm{X}(t_0)) + (t-t_0) f^{(1)}(t_0, \mathrm{X}(t_0)) + \frac{(t-t_0)^2}{2!} f^{(2)}(t_0, \zeta) \right) dt,$$

where $\zeta \in [t_0, t]$. The previous integral is evaluated as follows:

$$\int_{t_0}^{t_0+h} f(t, \mathrm{X}(t))dt = hf(t_0, \mathrm{X}(t_0)) + \frac{h^2}{2} f^{(1)}(t_0, \mathrm{X}(t_0)) + \frac{h^3}{6} f^{(2)}(t_0, \zeta). \tag{25}$$

Then, we utilize the Taylor series for the non-integrand functions in Eq (24). We briefly write the highest degree of h as follows:

$$\frac{qh^3}{2}\left[0.5 f^{(2)}(t_0, \zeta_l) + f^{(2)}(t_0, \zeta_{l'})\right], \tag{26}$$

where ζ_l, $\zeta_{l'} \in [a,b]$. Let

$$f^{(2)}(t, \zeta) = \max(\left| f^{(2)}(t, \zeta_l) \right|, \left| f^{(2)}(t, \zeta_{l'}) \right|),$$

and the above term is written as $\dfrac{3qh^3}{4} f^{(2)}(t_0, \zeta)$. Thus, according to Eq (24), the integration error has the form

$$\left| E(f) \right| \le q\mathrm{K}h^3, \tag{27}$$

for some constant $\mathrm{K} = -\dfrac{7}{12} f^{(2)}(t, \zeta)$.

Theorem 2. Assume that H2 holds. The numerical scheme (23) is conditionally stable.

Proof. For simplicity, we will briefly write $f(t, \mathrm{X}(t))$ as $f(\mathrm{X})$ and $\mathrm{X}(t_{s+1})$ as X_s. Let $\widetilde{\mathrm{X}}_0, \widetilde{\mathrm{X}}_s$ be the perturbations of X_0 and $\widetilde{\mathrm{X}}_s$, respectively. So, the proposed numerical approach is transformed as follows:

$$\mathrm{X}_{s+1}+\tilde{\mathrm{X}}_{s+1}=\mathrm{X}_0+\tilde{\mathrm{X}}_0+\left[0.5qh+(1-q)\right]f\left(\mathrm{X}_{s+1}+\tilde{\mathrm{X}}_{s+1}\right)+\sum_{l=0}^{s}qhf\left(\mathrm{X}_l+\tilde{\mathrm{X}}_l\right). \tag{28}$$

From (23) and (28), we get

$$\tilde{\mathrm{X}}_{s+1}=\tilde{\mathrm{X}}_0+\left[0.5qh+(1-q)\right]\left(f\left(\mathrm{X}_{s+1}+\tilde{\mathrm{X}}_{s+1}\right)-f\left(\mathrm{X}_{s+1}\right)\right)+\sum_{l=0}^{s}qh\left[f\left(\mathrm{X}_l+\tilde{\mathrm{X}}_l\right)-f\left(\mathrm{X}_l\right)\right], \tag{29}$$

where $|qh|<1$. Taking the norm for both sides in Eq (29) and utilizing the triangle inequality, we obtain

$$\begin{aligned}\left\|\tilde{\mathrm{X}}_{s+1}\right\| &\le \left\|\tilde{\mathrm{X}}_0\right\|+\left[1.5qh+1-q\right]\left\|f\left(\mathrm{X}_{s+1}+\tilde{\mathrm{X}}_{s+1}\right)-f\left(\mathrm{X}_{s+1}\right)\right\|+\sum_{l=0}^{s-1}qh\left\|f\left(\mathrm{X}_l+\tilde{\mathrm{X}}_l\right)-f\left(\mathrm{X}_l\right)\right\| \\ &\le \left\|\tilde{\mathrm{X}}_0\right\|+\left[1.5qh+1-q\right]L\left\|\tilde{\mathrm{X}}_{s+1}\right\|+qhL\sum_{l=0}^{s-1}\left\|\tilde{\mathrm{X}}_l\right\|.\end{aligned} \tag{30}$$

The inequality (30) is reduced to

$$\left[1-(1.5qh+1-q)L\right]\left\|\tilde{\mathrm{X}}_{s+1}\right\|\le\left\|\tilde{\mathrm{X}}_0\right\|+qhL\sum_{l=0}^{s-1}\left\|\tilde{\mathrm{X}}_l\right\|. \tag{31}$$

Setting $L<\dfrac{1}{1.5qh+1-q}$, we get

$$\left\|\tilde{\mathrm{X}}_{s+1}\right\|\le\Psi(q,h)\left\|\tilde{\mathrm{X}}_0\right\|+qhL\Psi(q,h)\sum_{l=0}^{s-1}\left\|\tilde{\mathrm{X}}_l\right\|, \tag{32}$$

where

$$\Psi(q,h)=\frac{1}{1-(1.5qh+1-q)L}.$$

So, for each h, there exists a constant K_h such that $1<\Psi(q,h)<\mathrm{K}_h$. Thus,

$$\left\|\tilde{\mathrm{X}}_{s+1}\right\|\le\mathrm{K}_h\left\|\tilde{\mathrm{X}}_0\right\|+qhL\mathrm{K}_h\sum_{l=0}^{s-1}\left\|\tilde{\mathrm{X}}_l\right\|.$$

Finally, the Gröwnwall inequality implies that $\left\|\tilde{\mathrm{X}}_{s+1}\right\|\le\mathrm{K}\left\|\tilde{\mathrm{X}}_0\right\|$, which completes the proof.

Theorem 3. Assume that H1 and H2 hold. The numerical scheme (23) is conditionally convergent of order three, that is,

$$\left\|\mathrm{X}(t_{s+1})-\mathrm{X}_{s+1}\right\|\le q\mathrm{K}\mathrm{K}_h h^3. \tag{33}$$

Proof. Let $\mathrm{X}(t_{s+1})$ and X_{s+1} represent the actual and approximate solution, respectively. So, we get

$$\begin{aligned}
\mathrm{X}(t_{s+1})-\mathrm{X}_{s+1} &= (1-q)\left[f(\mathrm{X}(t_{s+1}))-f(\mathrm{X}_{s+1})\right]-0.5qhf(\mathrm{X}_{s+1})+q\left[\int_0^{t_{s+1}} f(\mathrm{X}(t_l))dt-\sum_{l=0}^{s} hf(\mathrm{X}_l)\right]\\
&= (0.5qh+1-q)\left[f(\mathrm{X}(t_{s+1}))-f(\mathrm{X}_{s+1})\right]-0.5qhf(\mathrm{X}(t_{s+1}))\\
&\quad +q\left[\int_0^{t_{s+1}} f(\mathrm{X}(t_l))dt-\sum_{l=0}^{s} hf(t_l)\right]\\
&\quad +q\sum_{l=0}^{s} h[f(\mathrm{X}(t_l))-f(\mathrm{X}_l)].
\end{aligned}$$

According to the triangle inequality and the inequality (27), we get

$$\begin{aligned}
\left\|\mathrm{X}(t_{s+1})-\mathrm{X}_{s+1}\right\| &\le (0.5hq+1-q)L\left\|\mathrm{X}(t_{s+1})-\mathrm{X}_{s+1}\right\|+0.5qh\left\|f(\mathrm{X}(t_{s+1}))\right\|\\
&\quad +q\mathrm{K}h^3+qL\sum_{l=0}^{s} h\left\|\mathrm{X}(t_l)-\mathrm{X}_l\right\|\\
&= (0.5hq+1-q)L\left\|\mathrm{X}(t_{s+1})-\mathrm{X}_{s+1}\right\|\\
&\quad +q\mathrm{K}h^3+0.5qhL(\left\|\mathrm{X}(t_{s+1})\right\|+\kappa)+qL\sum_{l=0}^{s} h\left\|\mathrm{X}(t_l)-\mathrm{X}_l\right\|.
\end{aligned} \tag{34}$$

Since $0<q<1,\ 0\le h<1$ and $L<\dfrac{1}{1.5qh+1-q}$, then $(0.5hq+1-q)L<1$ and $0.5hqL<1$. Thus, the inequality (34) becomes

$$\left\|\mathrm{X}(t_{s+1})-\mathrm{X}_{s+1}\right\| \le q\Psi(q,h)\mathrm{K}h^3+qhL\Psi(q,h)\sum_{l=0}^{s}\left\|\mathrm{X}(t_l)-\mathrm{X}_l\right\|. \tag{35}$$

Hence, the result (33) is directly obtained by applying the Gröwnwall inequality to (35).

To show the consistency between the fractional system and its integer-order counterpart using the previous numerical algorithms, we fix the parameter values at the set $\Omega^{(1)}$ with step size of 0.01 and initial conditions $x(0)=0.1487, y(0)=0.1525, z(0)=0.4008, w(0)=1.0412\times10^{-15}$. The results are depicted in Figure 4, which shows the solutions of the integer-order system (red plot) and its fractional-order counterpart (blue plot) with q very close to one $(q=0.995)$. The figure shows that the fractional and integer-order models have consistent solutions for a wide time scale ($0\le t<450$), despite the use of two different numerical algorithms.

Now, the above-mentioned numerical algorithm (23) is coded and executed with diverse values of the memory parameter q, the set $\Omega^{(1)}$, and $h=0.01$ to demonstrate the variety of complex behaviors that exist in the fractional two-drug AMR system (6). In Figure 5, chaotic attractors appear when $q=0.99$ and $q=0.98$. This indicates that the dynamical behaviors of system (6) become completely unpredictable when the fractional parameter is close enough to one. In addition, the shape of the aforementioned types of chaotic attractors resembles the chaotic attractor of the system's integer-order counterpart. When $q<0.9$, the chaotic behaviors are removed because the system's trajectories are settled into stable attractors. This shows the effect of the model's memory on the system's dynamics that result in extended transients and delayed reactions with smaller q.

On the other hand, the bifurcation diagram in Figure 6 illustrates that the growth rate r plays an important role in driving the two-drug AMR system (6) toward nonlinear dynamics and chaos. Figure 6a,

illustrates that the coexistence of both susceptible and infected populations is highly unpredictable as the growth rate of the susceptible population varies between two and three, and q approaches one (i.e., when past experiences have a weak effect on the current populations' behaviors). However, when the memory parameter descends far from one, i.e., when past experiences gradually affect the current populations' behaviors, the coexistence of both susceptible and infected populations gradually becomes predictable (see Figure 6b,c). This means that the memory parameter has a stabilizing effect on the complex dynamics of the two-drug AMR model.

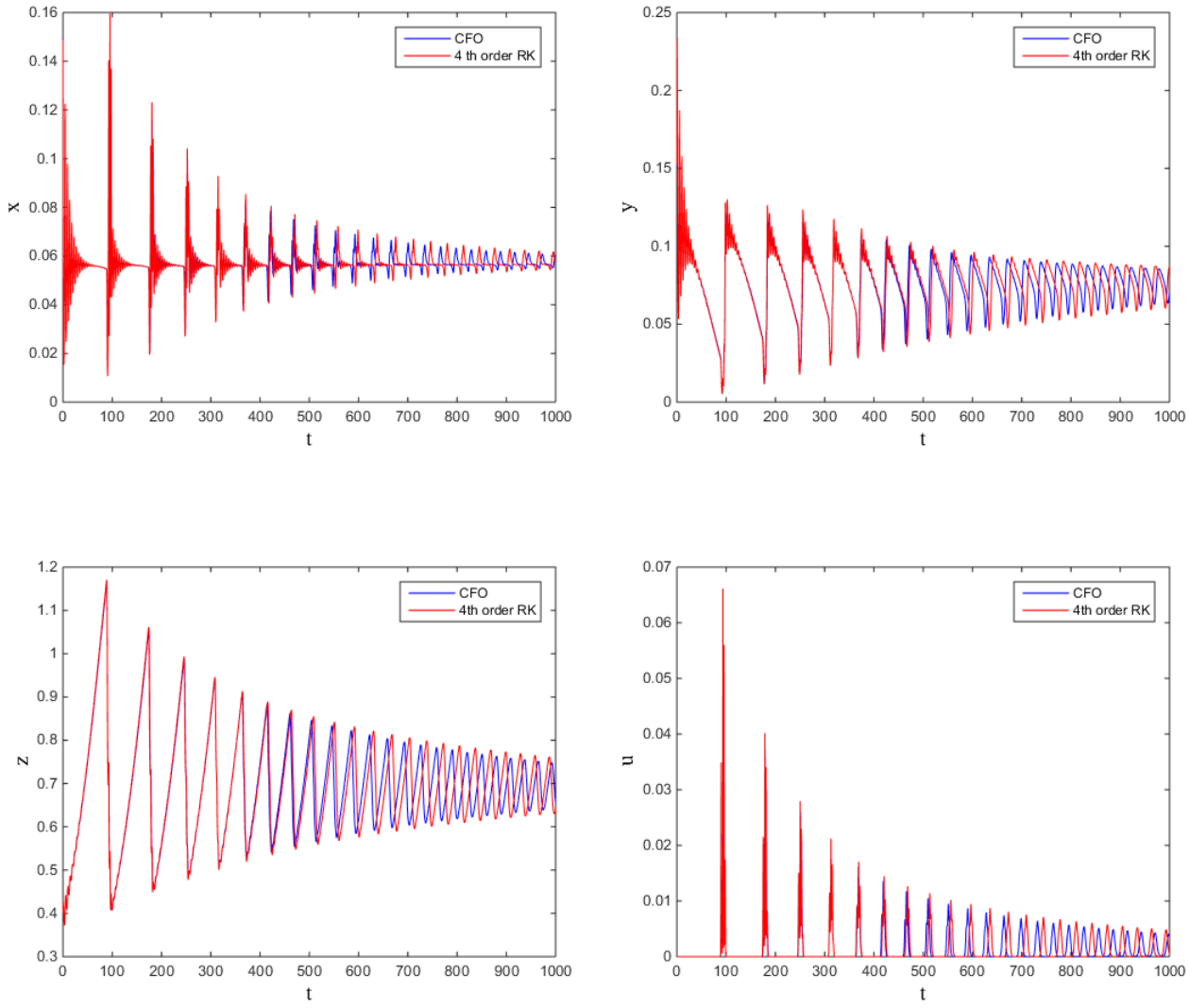

Figure 4. Solutions' components of the integer-order system (5) and the fractional-order system (6).

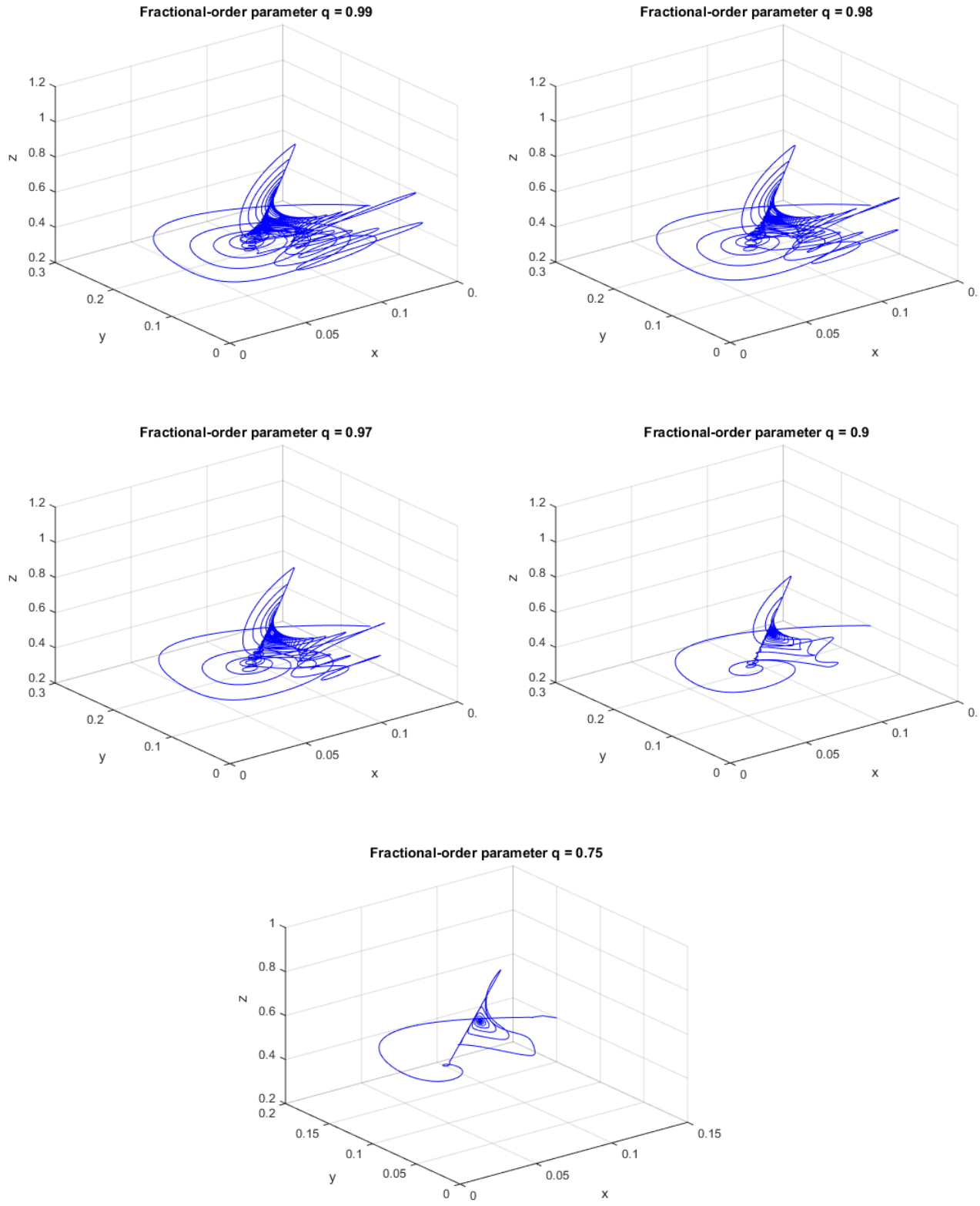

Figure 5. Variety of complex attractors of the two-drug AMR system (6), with initial values $x(0) = 0.1487, y(0) = 0.1525, z(0) = 0.4008, w(0) = 1.0412 \times 10^{-15}$ and using different values of q.

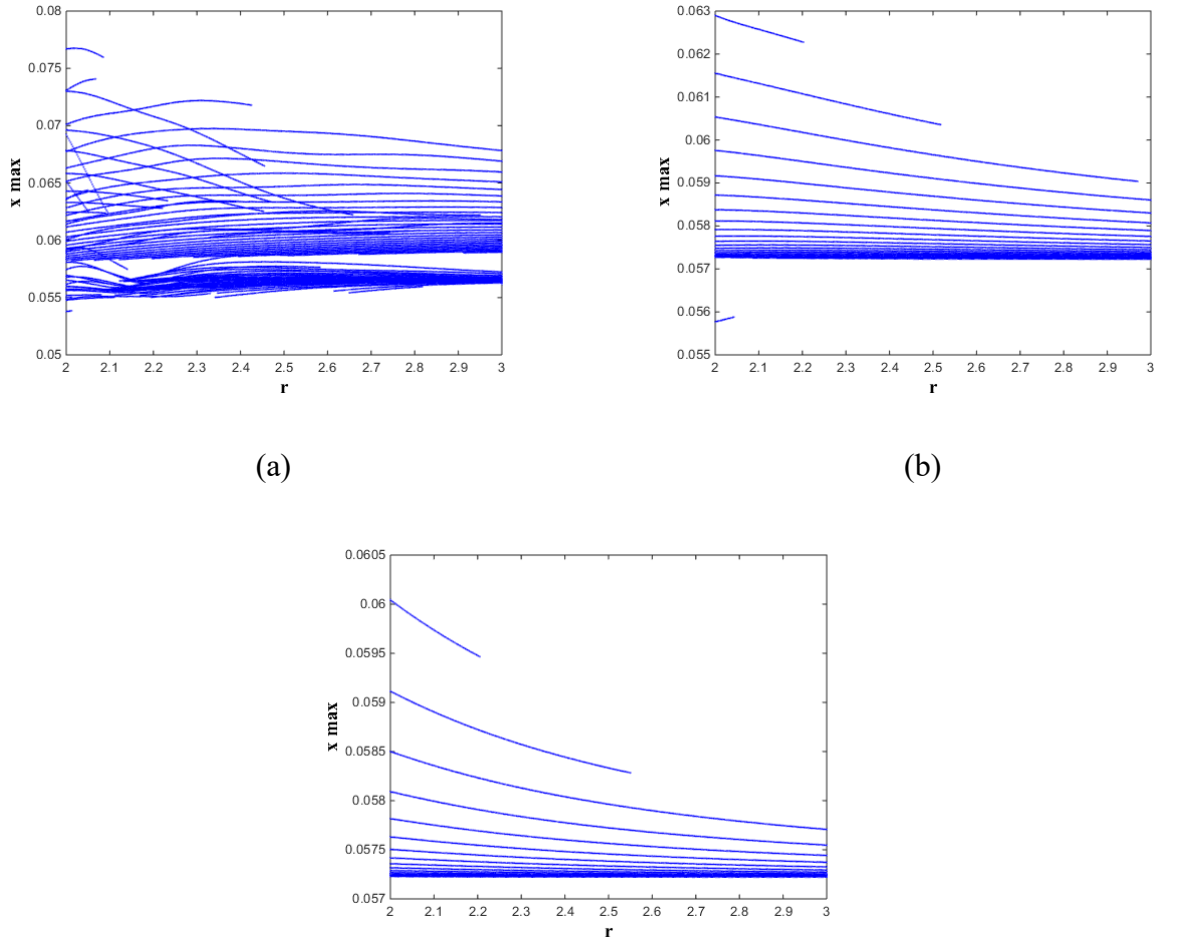

Figure 6. LM bifurcation diagram of the fractional two-drug AMR model (6) shown using $\Omega_r^{(1)}$ and with fractional-order: (a) $q = 0.999$, (b) $q = 0.9$, and (c) $q = 0.8$.

6. Conclusions

A two-drug antimicrobial resistance model governed by the CFO has been introduced. Based on the FRH criterion of differential systems governed by the CFO, the conditions of local stability of the drug-free, healthy, and multidrug resistance equilibrium states have been proven. The higher level of unpredictability between susceptible and infected populations has been illustrated via phase plots based on the numerical simulations, which have been carried out using a novel consistent algorithm for integrating fractional systems governed by the CFO. The conditional stability and convergence of the proposed numerical scheme have been proven. In addition, the novel numerical algorithm has been coded and implemented to obtain advanced software tools for examining complex dynamic behaviors such as the LM bifurcation diagrams and Lyapunov spectrum.

Using specific values of the indicated parameters, the effect of memory on stabilizing the complex dynamics in the considered model has been illustrated. It has been shown that when the memory becomes very weak ($q \approx 1$), the coexistence of both susceptible and infected populations is highly

unpredictable as the growth rate of the susceptible population varies between two and three. When experiences gradually affect the current populations' behaviors, the coexistence of both susceptible and infected populations gradually becomes predictable. Thus, linking the memory property of fractional operators with non-singular kernel to plausible biological mechanisms in AMR makes this modeling approach a better candidate to apply infection control strategies by limiting the spread or emergence of the drug-resistant bacteria. Moreover, the memory parameter may affect suitable treatment strategies because when q drops further to one, experiences gradually affect the current populations' behaviors, and so the coexistence of both susceptible and infected populations gradually becomes predictable. This makes the antimicrobial stewardship more effective by ensuring the appropriate, timely, and rational use of antibiotics to minimize resistance emergence.

Through such a modeling approach, the complex dynamics of some viral diseases can be estimated with higher accuracy, can be better understood, and can be successfully controlled, especially when recurrences of some severe viral diseases associated with MDR are observed.

Use of Generative-AI tools declaration

The author declares he has not used Artificial Intelligence (AI) tools in the creation of this article.

Acknowledgments

The author extends the appreciation to the Deanship of Postgraduate Studies and Scientific Research at Majmaah University for funding this research work through the project number (R-2026–126).

Conflict of interest

The author declares no conflict of interest in this paper.

References

1. I. Podlubny, *Fractional differential equations*, New York: Academic Press, 1999.
2. R. Hilfer, *Applications of fractional calculus in physics*, World Scientific, 2000. https://doi.org/10.1142/3779
3. J. J. Trujillo, E. Scalas, K. Diethelm, D. Baleanu, *Fractional calculus: models and numerical methods*, World Scientific, 2016.
4. N. Laskin, Fractional market dynamics, *Phys. A*, **287** (2000), 482–492. https://doi.org/10.1016/S0378-4371(00)00387-3
5. M. A. E. Herzallah, D. Baleanu, Fractional-order Euler-Lagrange equations and formulation of Hamiltonian equations, *Nonlinear Dyn.*, **58** (2009), 385–391. https://doi.org/10.1007/s11071-009-9486-z
6. N. Laskin, Time fractional quantum mechanics, *Chaos Soliton. Fract.*, **102** (2017), 16–28. https://doi.org/10.1016/j.chaos.2017.04.010
7. A. E. Matouk, *Advanced applications of fractional differential operators to science and technology*, IGI Global Scientific Publishing, 2020. https://doi.org/10.4018/978-1-7998-3122-8

8. A. E. Abouelregal, H. Ahmad, A modified thermoelastic fractional heat conduction model with a single-lag and two different fractional-orders, *J. Appl. Comput. Mech.*, **7** (2021), 1676–1686. https://doi.org/10.22055/jacm.2020.33790.2287
9. A. E. Matouk, Studying changes in the dynamical patterns in two physical models involving new Caputo operator, *J. Adv. Res.*, **67** (2025), 173–184. https://doi.org/10.1016/j.jare.2024.01.021
10. E. Ahmed, A. S. Elgazzar, On fractional order differential equations model for nonlocal epidemics, *Phys. A*, **379** (2007), 607–614. https://doi.org/10.1016/j.physa.2007.01.010
11. D. Baleanu, H. Mohammadi, S. Rezapour, A fractional differential equation model for the COVID-19 transmission by using the Caputo–Fabrizio derivative, *Adv. Differ. Equ.*, **2020** (2020), 299. https://doi.org/10.1186/s13662-020-02762-2
12. N. P. Dong, H. V. Long, A. Khastan, Optimal control of a fractional order model for granular SEIR epidemic with uncertainty, *Commun Nonlinear Sci. Numer. Simul.*, **88** (2020), 105312. https://doi.org/10.1016/j.cnsns.2020.105312
13. Z. Avazzadeh, H. Hassani, P. Agarwal, S. Mehrabi, M. J. Ebadi, M. S. Dahaghin, An optimization method for studying fractional-order tuberculosis disease model via generalized Laguerre polynomials, *Soft Comput.*, **27** (2023), 9519–9531. https://doi.org/10.1007/s00500-023-08086-z
14. A. Althemairi, F. Hussien, A. A. Farghaly, Dynamic study of a delayed fractional-order SEIR epidemic model with general incidence and treatment functions, *Appl. Math. Inf. Sci.*, **17** (2023), 35–47. https://doi.org/10.18576/amis/170106
15. F. A. Rihan, U. Kandasamy, H. J. Alsakaji, N. Sottocornola, Dynamics of a fractional-order delayed model of COVID-19 with vaccination efficacy, *Vaccines*, **11** (2023), 758. https://doi.org/10.3390/vaccines11040758
16. F. Evirgen, E. Ucar, S. Ucar, N. Ozdemir, Modelling Influenza A disease dynamics under Caputo-Fabrizio fractional derivative with distinct contact rates, *Math. Modell. Numer. Simul. Appl.*, **3** (2023), 58–73. https://doi.org/10.53391/mmnsa.1274004
17. A. E. Matouk, I. G. Ameen, Y. A. Gaber, Analyzing the dynamics of fractional spatio-temporal SEIR epidemic model, *AIMS Math.*, **9** (2024), 30838–30863. https://doi.org/10.3934/math.20241489
18. A. Padder, A. E. Matouk, S. Qureshi, K. Dehingia, T. Ul Rahman Shah, Analyzing the impact of single feedback control strategy on the dynamics of fractional order tumor model, *Discov. Appl. Sci.*, **7** (2025), 1301. https://doi.org/10.1007/s42452-025-07863-9
19. A. Padder, S. Qureshi, A. E. Matouk, K. Dehingia, Dynamical analysis of a vector-borne disease model with control function strategies, *Discov. Appl. Sci.*, **7** (2025), 1301. https://doi.org/10.1007/s42452-025-07644-4
20. J. M. Cruz-Duarte, J. Rosales-Garcia, C. R. Correa-Cely, A. Garcia-Perez, J. G. Avina-Cervantes, A closed form expression for the Gaussian–based Caputo–Fabrizio fractional derivative for signal processing applications, *Commun. Nonlinear Sci. Numer. Simul.*, **61** (2018), 138–148. https://doi.org/10.1016/j.cnsns.2018.01.020
21. M. Ran, X. Liao, D. Lin, R. Yang, Analog realization of fractional-order capacitor and inductor via the Caputo-Fabrizio derivative, *J Adv. Comput. Intell. Intell. Inform.*, **25** (2021), 291–300. https://doi.org/10.20965/jaciii.2021.p0291
22. D. Yu, X. Liao, Y. Wang, Modeling and analysis of Caputo-Fabrizio definition-based fractional-order Boost converter with inductive loads, *Fractal Fract.*, **8** (2024), 81. https://doi.org/10.3390/fractalfract8020081

23. A. M. Alqahtani, S. Sharma, A. Chaudhary, A. Sharma, Application of Caputo-Fabrizio derivative in circuit realization, *AIMS Math.*, **10** (2025), 2415–2443. https://doi.org/10.3934/math.2025113
24. A. E. Matouk, M. Botros, S. Kumar, A. B. Albidah, Hidden attractors, chaos control and synchronization in two fractional systems governed by Caputo-Fabrizio derivatives, *Discrete Dyn. Nat. Soc.*, **2025** (2025), 7471599. https://doi.org/10.1155/ddns/7471599
25. M. A. Khan, Z. Hammouch, D. Baleanu, Modeling the dynamics of hepatitis E via the Caputo–Fabrizio derivative, *Math. Model. Nat. Phenom.*, **14** (2019), 311. https://doi.org/10.1051/mmnp/2018074
26. E. J. Moore, S. Sirisubtawee, S. Koonprasert, A Caputo-Fabrizio fractional differential equation model for HIV/AIDS with treatment compartment, *Adv. Differ. Equ.*, **2019** (2019), 200. https://doi.org/10.1186/s13662-019-2138-9
27. D. Baleanu, A. Jajarmi, H. Mohammadi, S. Rezapour, A new study on the mathematical modelling of human liver with Caputo-Fabrizio derivative, *Chaos Soliton. Fract.*, **134** (2020), 109705. https://doi.org/10.1016/j.chaos.2020.109705
28. O. J. Peter, Transmission dynamics of fractional order Brucellosis model using Caputo-Fabrizio operator, *Int. J. Differ. Equ.*, **2020** (2020), 2791380. https://doi.org/10.1155/2020/2791380
29. E. Bonyah, M. Juga, Fractional dynamics of coronavirus with comorbidity via Caputo-Fabrizio derivative, *Commun. Math. Biol. Neurosci.*, **2022** (2022), 12.
30. Z. Shah, N. Ullah, R. Jan, M. H. Alshehri, N. Vrinceanu, E. Antonescu, et al., Existence and sensitivity analysis of a Caputo-Fabrizio fractional order vector-borne disease model, *Eur. J. Pure Appl. Math.*, **18** (2025), 5687. https://doi.org/10.29020/nybg.ejpam.v18i2.5687
31. R. Shafqat, A. Alsaadi, Bifurcation in a fractional SIR model with normalized Caputo-Fabrizio derivative, *Discrete Dyn. Nat. Soc.*, **2025** (2025), 4368999. https://doi.org/10.1155/ddns/4368999
32. R. Shafqat, A. Al-Quran, A. Alsaadi, A. M. Djaouti, Normalized Caputo-Fabrizio SVIR modeling and bifurcation analysis, *Sci. Rep.*, **16** (2026), 8193. https://doi.org/10.1038/s41598-026-38301-4
33. A. Wolf, J. B. Swift, H. L. Swinney, J. A. Vastano, Determining Lyapunov exponents from a time series, *Phys. D*, **16** (1985), 285–287. https://doi.org/10.1016/0167-2789(85)90011-9
34. N. Almutairi, S. Saber, On chaos control of nonlinear fractional Newton-Leipnik system via fractional Caputo-Fabrizio derivatives, *Sci. Rep.*, **13** (2023), 22726. https://doi.org/10.1038/s41598-023-49541-z
35. R. P. Chauhan, S. Kumar, B. S. T. Alkahtani, S. S. Alzaid, A study on fractional order financial model by using Caputo–Fabrizio derivative, *Results Phys.*, **57** (2024), 107335. https://doi.org/10.1016/j.rinp.2024.107335
36. A. Al-khedhairi, Dynamical analysis and chaos synchronization of a fractional-order novel financial model based on Caputo-Fabrizio derivative, *Eur. Phys. J. Plus*, **134** (2019), 532. https://doi.org/10.1140/epjp/i2019-12878-4
37. X. Liao, M. Ran, D. Yu, Y. Wang, D. Lin, Chaos control of fractional-order Buck converter based on Caputo-Fabrizio fractional derivative, *IECON 2023-49th Annual Conference of the IEEE Industrial Electronics Society*, 2023, 1–6. https://doi.org/10.1109/IECON51785.2023.10312608
38. M. M. El-Dessoky, M. A.Khan, Application of Caputo–Fabrizio derivative to a cancer model with unknown parameters, *Discrete Cont. Dyn. Syst.-S*, **14** (2021), 3557–3575. https://doi.org/10.3934/dcdss.2020429
39. A. E. Matouk, M. Botros, Hidden chaotic attractors and self-excited chaotic attractors in a novel circuit system via Grünwald–Letnikov, Caputo-Fabrizio and Atangana-Baleanu fractional operators, *Alex. Eng. J.*, **116** (2025), 525–534. https://doi.org/10.1016/j.aej.2024.12.064

40. M. A. Khan, The dynamics of a new chaotic system through the Caputo-Fabrizio and Atangana-Baleanu fractional operators, *Adv. Mech. Eng.*, **11** (2019), 1–12. https://doi.org/10.1177/1687814019866540
41. J. A. Lewnard, Y. H. Grad, Vaccine waning and mumps re-emergence in the United States, *Sci. Transl. Med.*, **10** (2018), eaao5945. https://doi.org/10.1126/scitranslmed.aao5945
42. WHO Report, WHO/EMP/IAU/2018.06, 2018. Available form: https://iris.who.int/server/api/core/bitstreams/7c098913-b83e-4e2a-b54b-6622224f1dcc/content.
43. M. A. Arepyeva, A. S. Kolbin, S. V. Sidorenko, R. Lawson, A. A. Kurylev, Y. E. Balykina, et al., A mathematical model for predicting the development of bacterial resistance based on the relationship between the level of antimicrobial resistance and the volume of antibiotic consumption, *J. Glob. Antimicrob. Resist.*, **8** (2017), 148–156. https://doi.org/10.1016/j.jgar.2016.11.010
44. M. F. Elettreby, E. Ahmed, Multi-drug antimicrobial resistance model, *Math. Meth. Appl. Sci.*, **43** (2020), 10462–10473. https://doi.org/10.1002/mma.6433
45. E. Ahmed, A. S. Elgazzar, A. Elsadany, Simple mathematical models of antimicrobial resistance, *J. Fract. Calc. Appl.*, **11** (2020), 22–25.
46. S. W. Olesen, Uses of mathematical modeling to estimate the impact of mass drug administration of antibiotics on antimicrobial resistance within and between communities, *Infect. Dis. Poverty*, **11** (2022), 75. https://doi.org/10.1186/s40249-022-00997-7
47. F. Durazzi, M. D. Pezzani, F. Arieti, O. Simonetti, L. M. Canziani, E. Carrara, et al., Modelling antimicrobial resistance transmission to guide personalized antimicrobial stewardship interventions and infection control policies in healthcare setting: a pilot study, *Sci. Rep.*, **13** (2023), 15803. https://doi.org/10.1038/s41598-023-42511-5
48. S. K. Ahmed, S. Hussein, K. Qurbani, R. H. Ibrahim, A. Fareeq, K. A. Mahmood, et al., Antimicrobial resistance: impacts, challenges, and future prospects, *J. Med. Surg. Public Health*, **2** (2024), 100081. https://doi.org/10.1016/j.glmedi.2024.100081
49. E. Ahmed, A. E. Matouk, Complex dynamics of some models of antimicrobial resistance on complex networks, *Math. Meth. Appl. Sci.*, **44** (2021), 1896–1912. https://doi.org/10.1002/mma.6889
50. G. A. M. B. Nchama, Properties of Caputo-Fabrizio fractional operators, New Trends Math Sci., **8** (2020), 1–25. https://doi.org/10.20852/ntmsci.2020.393
51. G. A. M. Nchama, L. D. Lau-Alfonso, A. M. L. Mecıas, M. R. Ricard, Properties of the Caputo-Fabrizio fractional derivative, *Appl. Math. Inf. Sci.*, **14** (2020), 761–769. https://doi.org/10.18576/amis/140503
52. H. Li, J. Cheng, H. B. Li, S. M. Zhong, Stability analysis of a fractional-order linear system described by the Caputo-Fabrizio derivative, *Mathematics*, **7** (2019), 200. https://doi.org/10.3390/math7020200
53. A. E. Matouk, Fractional Routh-Hurwitz conditions and nonlinear dynamics in some 3D and 4D dynamical systems modeled by Caputo-Fabrizio operators, *Res. Appl. Math.*, **26** (2025), 100588 https://doi.org/10.1016/j.rinam.2025.100588
54. T. Abdeljawad, D. Baleanu, On fractional derivatives with exponential kernel and their discrete versions, *Rep. Math. Phys.*, **80** (2017), 11–27. https://doi.org/10.1016/S0034-4877(17)30059-9

©2026 the Author(s), licensee AIMS Press. This is an open access article distributed under the terms of the Creative Commons Attribution License (https://creativecommons.org/licenses/by/4.0)